

Domain Structures in Monoclinic $\text{Pb}[(\text{Zn}_{1/3}\text{Nb}_{2/3})_{0.91}\text{Ti}_{0.09}]\text{O}_3$ Poled Single Crystals

Alexandra-Evelyne RENAULT^{1,2}, Hichem DAMMAK^{1*}, Gilbert CALVARIN¹, Mai PHAM THI^{2†} and Philippe GAUCHER²

¹Laboratoire Structures, Propriétés et Modélisation des Solides UMR 8580 CNRS, Ecole Centrale de Paris, 92295 Châtenay-Malabry, France

²THALES RESEARCH & TECHNOLOGY FRANCE, 91404 Orsay Cedex, France

(Received January 7, 2002; accepted for publication March 12, 2002)

A tetragonal (T) \leftrightarrow monoclinic (M) phase transition characterized by a wide thermal hysteresis is observed in $\text{Pb}[(\text{Zn}_{1/3}\text{Nb}_{2/3})_{0.91}\text{Ti}_{0.09}]\text{O}_3$ (PZN–9%PT) single crystals close to the morphotropic composition PZN–9%PT. The domain structure of crystals, determined by X-ray diffraction and optical observations, is dependent on the poling crystallographic direction. A monoclinic quasi-single domain structure is obtained by poling along the pseudocubic $[10\bar{1}]$ direction whereas an unexpected monoclinic multidomain state with macroscopic 2 mm symmetry can be obtained for $[001]$ poled crystals. Finally it is shown that the largest piezoelectric response corresponds to the monoclinic multidomain state of $[001]$ poled crystals. [DOI: 10.1143/JJAP.41.3846]

KEYWORDS: PZN–9%PT single crystal, X-ray diffraction, monoclinic phase, piezoelectricity, domain engineering

1. Introduction

The ultrahigh piezoelectricity of single crystals $\text{Pb}[(\text{Zn}_{1/3}\text{Nb}_{2/3})_{0.91}\text{Ti}_{0.09}]\text{O}_3$ (PZN–9%PT) close to the morphotropic phase boundary (MPB) has been reported.^{1–3} The material undergoes two successive phase transitions during a zero-field-heating-after-field-cooling run (ZFHFC)² (i) from cubic $m\bar{3}m$ to tetragonal 4 mm near 451 K and (ii) from tetragonal to rhombohedral 3 m near 341 K. Furthermore, Fujishiro *et al.*,⁴ using a (111) crystal plate under a polarizing microscope at the spontaneous state, observed a lower symmetry phase (monoclinic or triclinic) at the phase boundary between the tetragonal and rhombohedral phases. Fu et Cohen⁵ reported that the high piezoelectric response in the rhombohedral composition PZN–PT close to the MPB is due to the polarization rotation, between the rhombohedral and tetragonal phases via the monoclinic phase, during poling under an electric field applied along the pseudocubic $[001]$ direction. Later Noheda *et al.*⁶ showed that in PZN–8%PT the spontaneous rhombohedral phase is irreversibly transformed into the monoclinic phase during an electric field increase and the crystal comprises four domain variants corresponding to a macroscopic 4 mm symmetry. Recently, Cox *et al.*⁷ showed that the phase of PZN–9%PT (grounding of a poled crystal) is orthorhombic.

In this paper, we report new results for the domain structures and phases of PZN–9%PT single crystals poled along the two pseudocubic directions $[001]$ and $[10\bar{1}]$.

2. Experimental

PZN–9%PT single crystals were grown by the self flux method using a PbO flux.^{1,2,8–10} The flux and the PZN–PT raw materials were mixed at a PZN–9%PT: flux ratio of 45/55 (mol%). A total amount of 550 g of materials was placed in a 133 cm³ platinum crucible. The crucible was covered with a lid after two pre-melts at 1173 K for 2 h and then placed in a 346 cm³ Al₂O₃ crucible. The Al₂O₃ crucible was covered with a lid, to prevent both lead evaporation and damage to the electric furnace. The crucible was then placed in a computer-controlled electric furnace. The temperature was increased to 1463 K and maintained there for 2 h. It was reduced to 1173 K at 1 K/h. The size of the largest as-grown

crystal was approximately $10 \times 10 \times 8$ mm³. Crystals were cut and polished, with orientations $[100]/[010]/[001]$ (A and A'), $[101]/[010]/[10\bar{1}]$ (B) and $[11\bar{2}]/[1\bar{1}0]/[111]$ (C). The size of single crystals were $2.6 \times 2.6 \times 1.8$ (A), $1.7 \times 1.7 \times 3.6$ (A'), $1.6 \times 2.9 \times 1.6$ (B) and $4.2 \times 1.9 \times 0.9$ (C) mm³. Thin films of Cr/Au electrodes (~ 1300 Å) were sputtered on the (001), (10 $\bar{1}$) or (111) faces. The homogeneity of the samples was controlled by dielectric susceptibility measurements as a function of temperature using a LF impedance analyzer (HP-4192A). The Curie temperature T_C measured during the zero-field-cooling runs (ZFC) was equal to 449 ± 0.5 K. Samples were then poled either under a dc field at room temperature (RT) or during field cooling (FC). The piezoelectric properties were determined according to the IRE standard methods. X-ray diffraction experiments were performed on a high-accuracy two-axes diffractometer using Cu-K β monochromatic radiation issued from a Rigaku rotating anode (RU300, 18 kW). Single crystals were fixed on a copper sample holder mounted on a HUBER goniometric head. In the Bragg-Brentano geometry, the diffraction angles were measured with a precision relatively better than 0.002° (2θ). Two-dimensional maps of the diffracted intensity were also constructed by rotating step by step the crystal around the ω -axis. Such 2θ - ω mappings allowed disclosure and characterization of the domain structure of crystals.

3. Results

3.1 Dielectric properties

Figure 1(a) shows the temperature dependence of the piezoelectric permittivity $\epsilon_{33}^T/\epsilon_0$ along $[001]$ for crystal A, along $[10\bar{1}]$ for crystal B and along $[111]$ for crystal C, at 10 kHz and for a 100 kV/m applied field in FC. For crystals A and B, two anomalies are observed at 451 K and 300 K, corresponding respectively to the cubic (C) \rightarrow tetragonal (T) and to the tetragonal (T) to monoclinic⁶ (M) (or orthorhombic⁷ (O)) phase transitions. The low value of $\epsilon_{33}^T/\epsilon_0$ (~ 1800) along $[001]$ in the 300–450 K temperature range is due to the formation of a tetragonal single domain under the dc bias field. On the other hand, when the electric field is applied along $[10\bar{1}]$, the formation of adjacent 90° domains (2T state) leads to a larger value of $\epsilon_{33}^T/\epsilon_0$ (~ 15000) in the same temperature range. An opposite effect is observed below 300 K and $\epsilon_{33}^T/\epsilon_0$ along $[10\bar{1}]$ is strongly reduced

*E-mail address: dammak@spms.ecp.fr

†E-mail address: mai.phamthi@thalesgroup.com

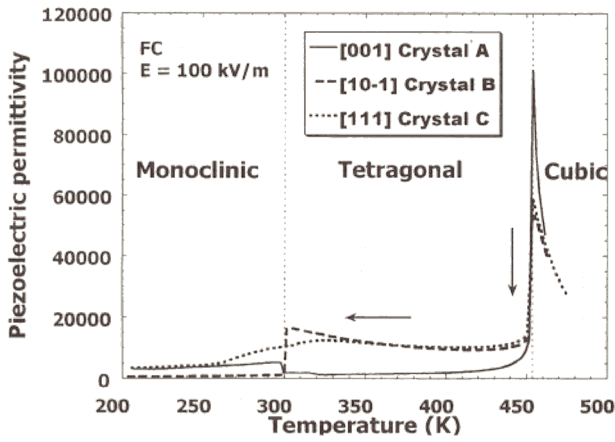


Fig. 1. Temperature dependence of piezoelectric permittivity $\epsilon_{33}^T/\epsilon_0$ measured at 10 kHz in a FC process ($E = 100 \text{ kV/m}$) for [001], [10 $\bar{1}$] and [111] poling directions.

showing that a “single domain crystal” is obtained, the component of its polar axis is close to the [10 $\bar{1}$] direction.

When the electric field is applied along [111], the large values of $\epsilon_{33}^T/\epsilon_0$ measured at all temperatures show that the crystal remains in a multidomain state. In fact, $\epsilon_{33}^T/\epsilon_0$ values are equal to those measured along [10 $\bar{1}$] in the 2T state (i.e., 300–450 K temperature range) and equal to those measured along [001] in the 200–300 K temperature range. In the following, we show that at room temperature the domain symmetry is monoclinic (M) for both [001] and [10 $\bar{1}$] poling directions.

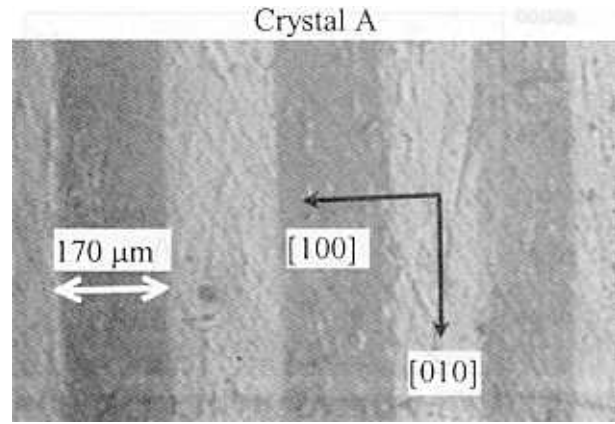
3.2 Monoclinic domains in [001] poled crystals

Optical observations of crystal A poled along [001] show bands parallel to [010] when light is reflected on (001) or (100) face [Figs. 2(a) and 2(b)] and a dense striated aspect along [001] when light is transmitted along [010]. These observations indicate that the domain arrangements along [100] and [010] seem to be different. On the other hand, the (004), (040) and (400) diffraction peaks, respectively recorded on the three faces of crystal A, are unique [Fig. 3(a)] and correspond to three different reticular distances. A $2\theta-\omega$ mapping, carried out in the (a^* , c^*) reciprocal plane around (400), shows two maxima centered at the same 2θ [Fig. 3(b)]. A similar peak splitting was also observed in the mapping carried out around (004). The value of splitting $\Delta\omega = 0.34^\circ$ is directly correlated to the angle between adjacent domains. The optical observations as well as the X-ray records indicate that crystal A comprises two families of monoclinic domains (2M). The orientation relationships (OR) between the $m1$ and $m2$ families are shown as follows:

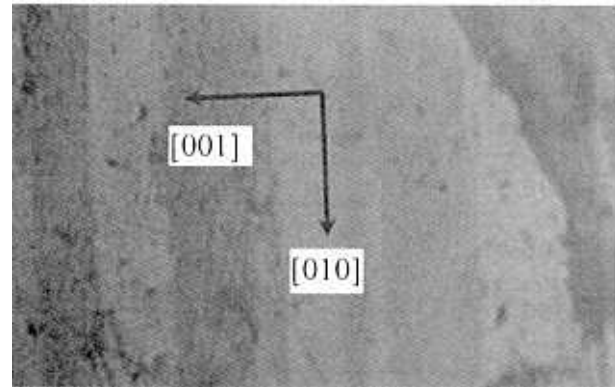
- (I): $[001]_{m1} \parallel [001]_{m2}$ and $(010)_{m1} \parallel (0\bar{1}0)_{m2}$, for the (001) face [Fig. 5(a)].
- (II): $[100]_{m1} \parallel [\bar{1}00]_{m2}$ and $(010)_{m1} \parallel (0\bar{1}0)_{m2}$, for the (100) face [Fig. 5(b)].

These two ORs are very similar and they correspond probably to two types of local relaxation inside the crystal in order to minimize the elastic and electric energies of the poled crystal.

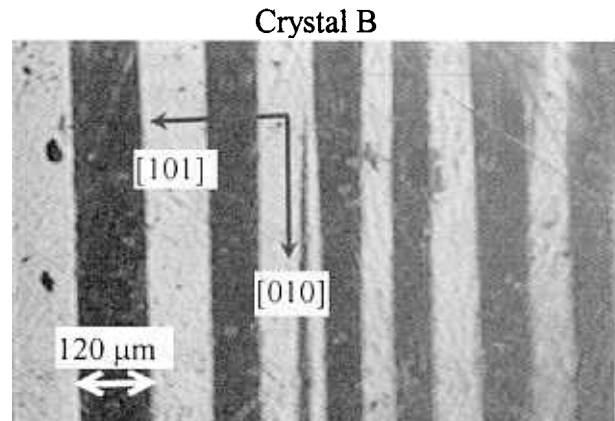
The lattice parameters of the monoclinic cell, calculated from the experimental (2θ) values of (400), (040), (004) and with $\beta = 90^\circ + \Delta\omega/2$, are



(a) (001) plane



(b) (100) plane



(c) (10 $\bar{1}$) plane

Fig. 2. Optical observations of domains in crystal A: (a) (001) plane, (b) (100) plane, and in crystal B: (10 $\bar{1}$) plane.

$$\begin{aligned} a_m &= 4.0635(4), \\ b_m &= 4.0290(4), \\ c_m &= 4.0674(4) \text{ \AA} \end{aligned}$$

and

$$\beta = 90.17(2)^\circ.$$

A different monoclinic domain state (four-domain state, 4M) was also obtained on another crystal A' (similar to crystal A). Figure 3(c) shows that the (303) diffraction peak, recorded from the crystal A' oriented [010] \parallel ω -axis, is a

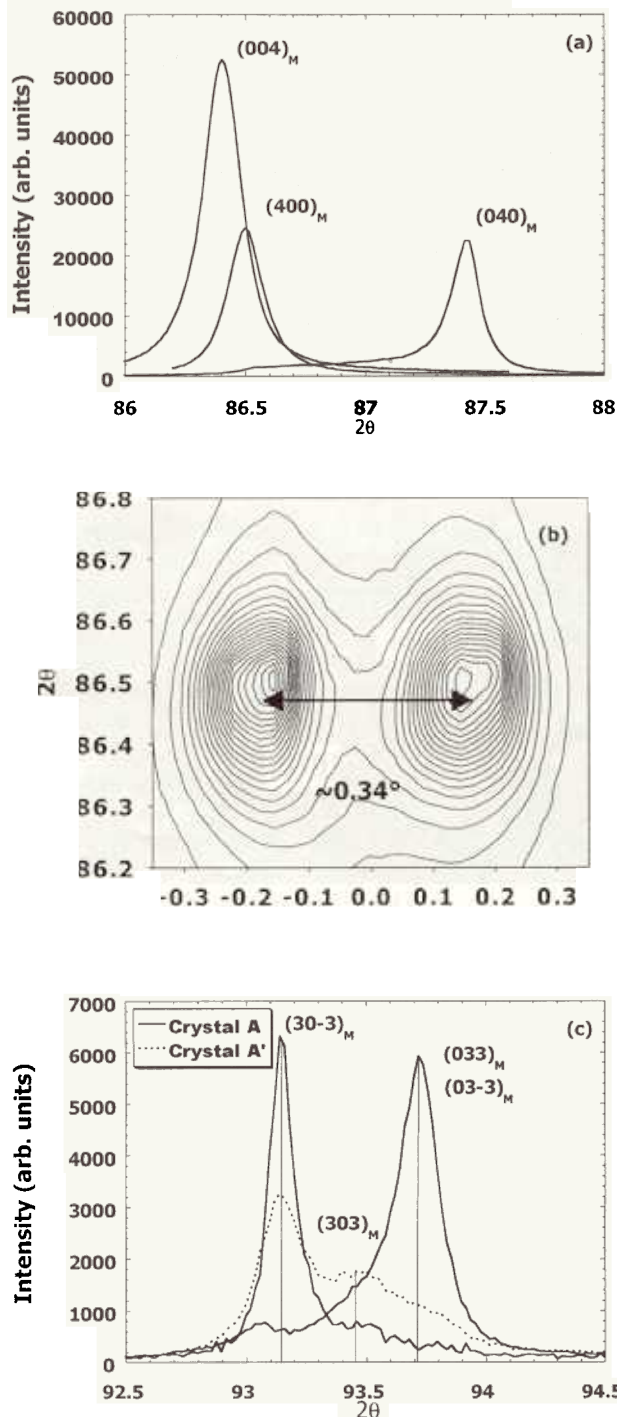


Fig. 3. X-ray diffraction patterns for crystals A and A' poled along [001]: (a) $(400)_M$ diffraction peaks recorded on three faces of crystal A, (b) 2θ - ω mapping in the (a^*, c^*) reciprocal plane carried out around the (400) reflection for crystal A, (c) $\{303\}$ diffraction peaks recorded from crystal A (solid line) and from crystal A' (dotted line).

triplet. Under the same diffraction conditions, one single peak $(30\bar{3})$ was obtained for crystal A (2M state). A second peak, (033) or $(03\bar{3})$, corresponds to a second recording carried out from the same crystal oriented $[100] \parallel \omega$ -axis. Therefore, the components of the triplet of crystal A' can be indexed, using the monoclinic cell parameters determined on crystal A, as $(30\bar{3})_{m1}$, $(30\bar{3})_{m2}$ and $(033)_{m3}$.

3.3 Monoclinic quasi-single domain in $[10\bar{1}]$ poled crystal

Optical observations of crystal B poled along $[10\bar{1}]$ show

also bands parallel to $[010]$ when light is reflected on the $(10\bar{1})$ face [Fig. 2(c)]. On the other hand, 2θ - ω mappings carried out in the (a^*, c^*) reciprocal plane, around $(30\bar{3})$ [Fig. 4(a)], $(00\bar{5})$ [Fig. 4(b)] and $(30\bar{4})$ present two maxima. The two components of $(30\bar{3})$, which are separated by an angle of about 0.036° in ω , have the same $2\theta_{\max}$ (i.e., the same reticular distance) [Fig. 4(a)] whereas the two components of $(00\bar{5})$ have different reticular distances [Figs. 4(b) and 4(d)].

The optical observations and the peak splittings on X-ray mappings suggest that crystal B comprises two domain families. This polydomain state is not consistent with an orthorhombic symmetry; indeed, in this symmetry, the polar axis is very close to the pseudocubic direction $[10\bar{1}]$ involving to the formation of a single domain state. On the other hand, with a monoclinic symmetry (i.e., a and c are different), two domain families $m1$ and $m2$ are possible. From a domain to another, a_m and c_m are exchanged and the $[101]_m$ direction is rotated by about 0.036° [Fig. 5(d)]. The OR between the two monoclinic domains is shown as follows

$$(III): [10\bar{1}]_{m1} \parallel [10\bar{1}]_{m2} \text{ and } (010)_{m1} \parallel (0\bar{1}0)_{m2}.$$

The differences between the reticular distances of $(00\bar{5})$ and (500) as well as the $(30\bar{3})$ peak splitting ($\Delta\omega = 0.036^\circ = 6.3 \times 10^{-4}$ rad) are quite consistent with the OR: $[10\bar{1}]_{m1} \parallel [10\bar{1}]_{m2}$. Indeed, the angle calculated between the planes $(30\bar{3})_{m1}$ and $(30\bar{3})_{m2}$ is approximately¹¹⁾ equal to

$$2 \times \left(\frac{c_m}{a_m} - 1 \right) = 2 \times \left(\frac{d_{00\bar{5}}^m}{d_{500}^m} - 1 \right) = 6.2(2) \times 10^{-4} \text{ rad.}$$

This value is close to $\Delta\omega = 6.3 \times 10^{-4}$ rad.

In order to determine the monoclinic lattice parameters, several diffraction peaks: $(30\bar{3})$, $(33\bar{3})$, $(24\bar{2})$, $(30\bar{4})$, $(40\bar{3})$, $(00\bar{5})$, (500) , (303) , and (204) were recorded by orienting the crystal along three different directions: $[101]$, $[010]$ and $[10\bar{1}]$. The values of monoclinic parameters, calculated from a least-square refinement of experimental d_{hkl} , are the following:

$$a_m = 4.0617(1) \text{ \AA.}$$

$$b_m = 4.027(2) \text{ \AA,}$$

$$c_m = 4.0628(1) \text{ \AA}$$

and

$$\beta = 90.19(2)^\circ$$

The values of a_m and c_m are very close, so a 2-fold orthorhombic cell was also considered. A good fit (error less than 5×10^{-4}) was also obtained with

$$a_o = 5.754(1),$$

$$b_o = 4.027(2)$$

and

$$c_o = 5.736(1) \text{ \AA.}$$

As expected, the pseudocubic parameter $\frac{1}{2} \times \sqrt{a_o^2 + c_o^2} = 4.062(1) \text{ \AA}$ has a value intermediate between a_m and c_m .

4. Discussion and Conclusions

PZN-9%PT single crystals, poled under a low electric field ($E = 100 \text{ kV/m}$), are monoclinic at room temperature.

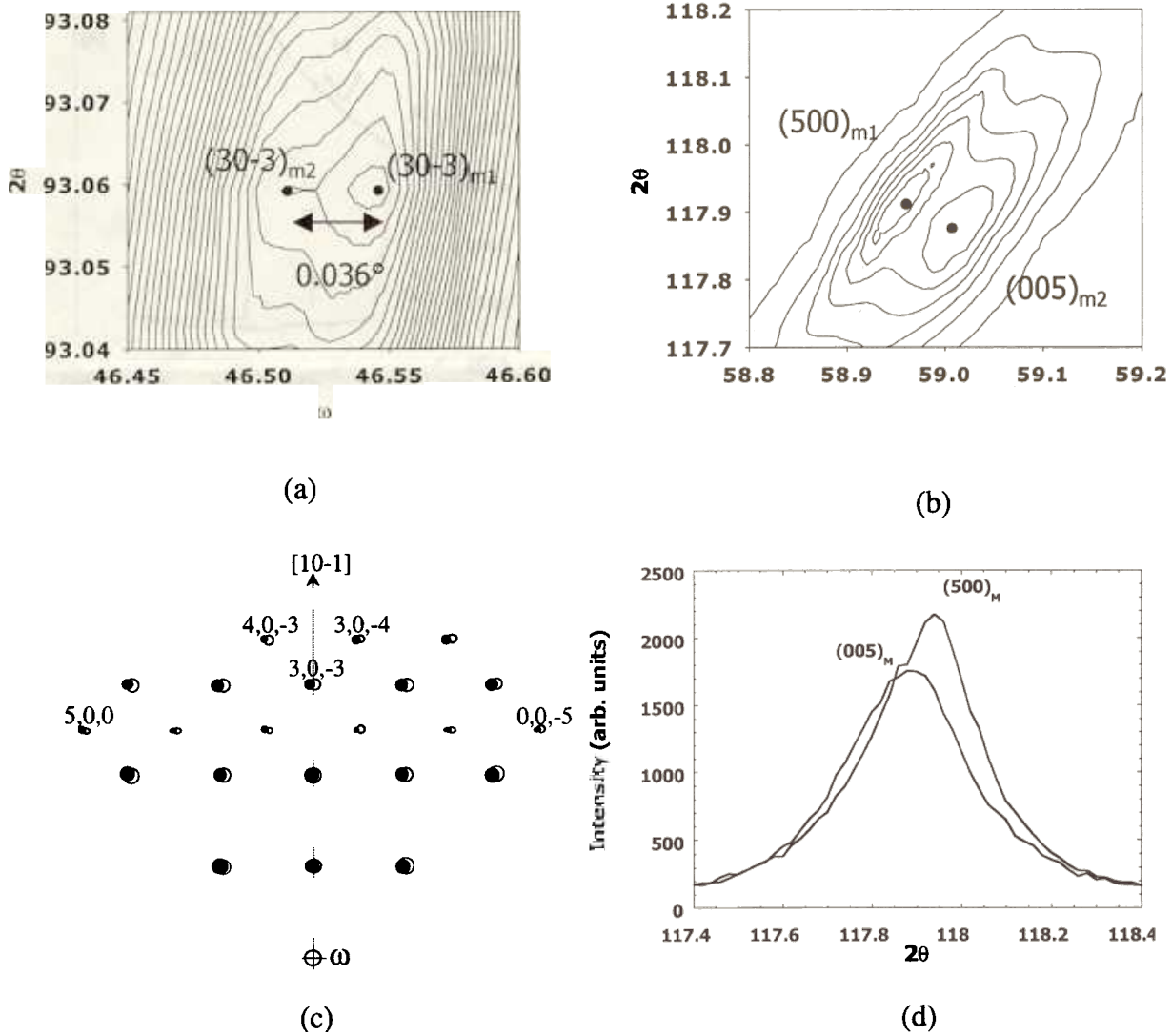


Fig. 4. X-ray diffraction data from crystal B poled along $[10\bar{1}]$: (a) and (b) 2θ - ω mappings in the (a^*, c^*) reciprocal plane carried out around the $(30\bar{3})$ and (005) reflections, respectively, (c) (a^*, c^*) reciprocal plane showing the superposition of $(h0\bar{l})_{m1}$ and $(l0\bar{h})_{m2}$ reflections resulting from monoclinic domains $m1$ and $m2$ that have the $[10\bar{1}]$ direction in common, (d) pattern showing that $(005)_M$ and $(500)_M$ peaks have different reticular distances.

The monoclinic symmetry was confirmed by the 2θ - ω mappings which allow us to distinguish between domains in the crystal. However, optical observations, dielectric and high-resolution X-ray measurements show that poled crystals can adopt different monoclinic domain structures according to the direction of the poling field. A monoclinic quasi-single domain (1M) was obtained for the first time by poling the crystal along the pseudocubic $[10\bar{1}]$ direction. The crystal is not strictly single domain because the polar axis of the monoclinic phase makes an angle of a few degrees with the poling $[10\bar{1}]$ direction. When crystal is poled along $[001]$, a more complex monoclinic domain state is obtained, because the polar axis makes an angle of about 45° with the poling direction. Two different domain states were obtained: a two-domain state (2M) with crystal A and a four-domain state (4M) with crystal A'. The existence of two different states could be related to the different domain configurations for crystals A and A' before poling.

The 4M configuration (macroscopic 4 mm symmetry) of monoclinic domains is the most common configuration; this configuration was recently evidenced by Noheda *et al.*⁶⁾ in

PZN-8%PT. Since the electromechanical and dielectric properties depend on the macroscopic symmetry of the crystal, in the 4M configuration the transverse directions: $[100]$ and $[010]$ are equivalent. On the other hand, the 2M configuration (macroscopic 2 mm symmetry) is unexpected because it leads to two nonequivalent transverse directions: $[100]$ and $[010]$, this macroscopic anisotropy involves that the d_{31} and d_{32} constants are not equal. Therefore, to obtain a maximal piezoelectric response in the transverse mode the longitudinal wave propagation should be parallel to the vector a_m contributing to the polar vector, but not to b_m .

The piezoelectric properties of crystal A' were measured as a function of temperature, apart from the $M \leftrightarrow T$ phase transition, in order to relate them to the symmetry of the phase and to the domain configuration. Figure 6(a) shows that the $M \leftrightarrow T$ transition is characterized by a wide hysteresis when the temperature is cycled between 280 K and 360 K. An abrupt change of the piezoelectric permittivity occurs at temperatures of the $M \rightarrow T$ and $T \rightarrow M$ transitions. Furthermore, Fig. 6(b) shows that for $[001]$ poled crystals the piezoelectric coefficient d_{33} and the electro-

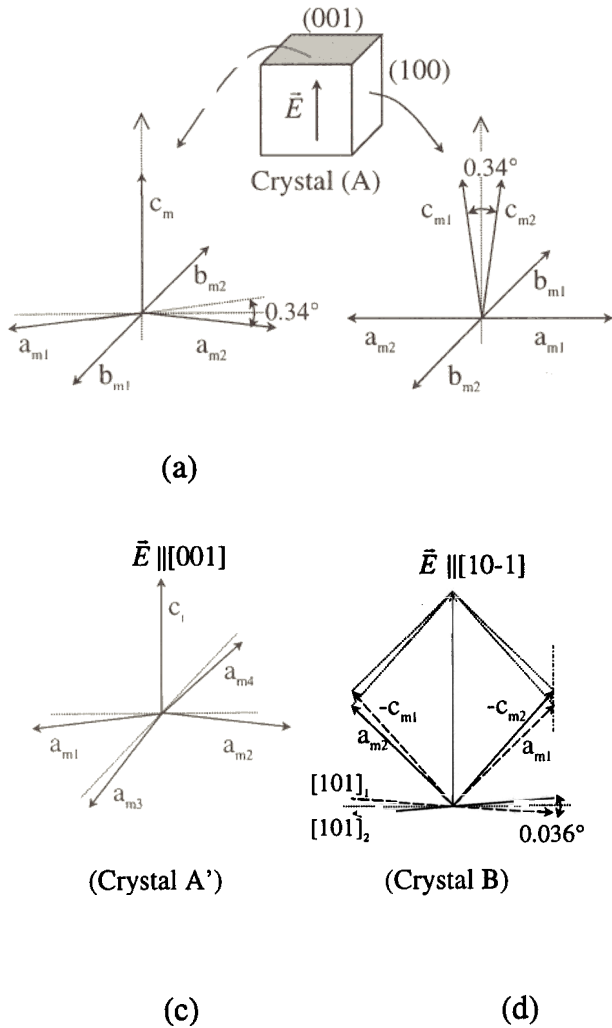


Fig. 5. Schematic representation of orientation relationships between crystallographic axes of monoclinic domains for crystal A: (a) and (b), crystal A': (c) and crystal B: (d).

mechanical coupling factor k_{33} are larger in the monoclinic multidomain state than in the tetragonal single-domain state. These results confirm unambiguously that the monoclinic phase and its multidomain structures are responsible for the exceptional piezoelectric response in PZN-9%PT. Such a behavior was already reported in KNbO_3 .¹²⁾

Acknowledgments

The authors are grateful to M. Gramond, J. Chevreul and B. Fraisse for helping during X-ray diffraction experiments and electrical measurements.

1) J. Kuwata, K. Uchino and S. Nomura: *Ferroelectrics* **37** (1981) 579.
 2) J. Kuwata, K. Uchino and S. Nomura: *Jpn. J. Appl. Phys.* **21** (1982)

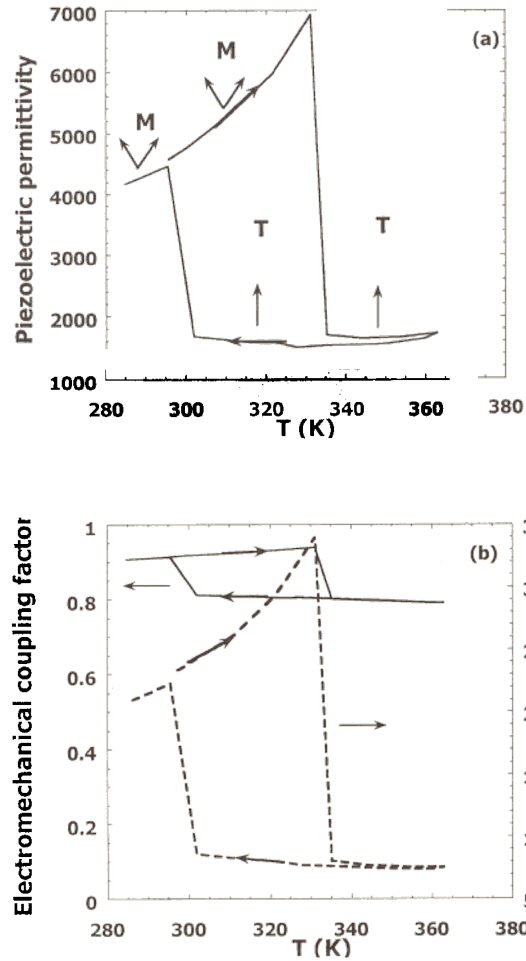


Fig. 6. Temperature dependence of (a) piezoelectric permittivity $\epsilon_{33}^T/\epsilon_0$, (b) piezoelectric constant d_{33} and electromechanical coupling factor k_{33} , for crystal A' poled along [001].

1298.
 3) S. E. Park and T. R. Shrout: *J. Appl. Phys.* **82** (1997) 1804.
 4) K. Fujishiro, R. Vlokh, Y. Uesu, Y. Yamada, J. M. Kiat, B. Dkhil and Y. Yamashita: *Jpn. J. Appl. Phys.* **37** (1998) 5246.
 5) H. Fu and R. E. Cohen: *Nature (London)* **403** (2000) 281.
 6) B. Noheda, D. E. Cox, G. Shirane, S. E. Park, L. E. Park, L. E. Cross and Z. Zhong: *Phys. Rev. Lett.* **86** (2001) 3891.
 7) D. E. Cox, B. Noheda, G. Shirane, Y. Uesu, K. Fujishiro and Y. Yamada: *Appl. Phys. Lett.* **79** (2001) 400.
 8) F. J. Kumar, L. C. Lim, C. Chilong and M. J. Tan: *J. Cryst. Growth* **216** (2000) 311.
 9) T. Kobayashi, S. Shimanuki, S. Saitoh and Y. Yamashita: *Jpn. J. Appl. Phys.* **36** (1997) 6035.
 10) S. Gentil, G. Robert, N. Setter, P. Tissot and J. P. Rivera: *Jpn. J. Appl. Phys.* **39** (2000) 2732.
 11) The angle between $(10\bar{1})_{m1}$ and $(10\bar{1})_{m2}$ is twice that between $[10\bar{1}]_m$ and $(10\bar{1})_m$ and its expression is simplified by using $\sin(\beta) \approx 1$ and $c_m^2 - a_m^2 \approx 2a_m(c_m - a_m)$.
 12) S. Wada, A. Seike and T. Tsurumi: *Jpn. J. Appl. Phys.* **40** (2001) 5690.